

FRACTURE ANALYSIS OF EPOXY-ALUMINUM ADHESIVE JOINT EXPOSED TO THERMAL AND STRUCTURAL LOADS

J. Korbel*, J. Klusák, Z. Knésl****

Summary: *The paper presents a fracture mechanics approach to estimation of critical load (thermal or structural) of adhesive joints. Attention is focused on failure of test specimens prepared by gluing aluminum plates with a commercial thermosetting adhesive. Residual stresses caused by differences of thermal expansion of the adhesive and adherent are also examined. Classical fracture mechanics does not deal with behavior of a bi-material interface, and therefore an approach based on a generalized stress intensity factor and generalized fracture toughness is employed.*

1. Introduction

Adhesive joints are occasionally used for assemblies of ABB products. Due to long term reliability requirements it is necessary to assure perfect adhesion between parts when exposed to thermal and structural loads during operational life. One of the main reasons for damage of adhesive joints is the presence of singular stress concentrators at the free edge of the interface between adhesives and adherents. The concentrators are modeled using a bi-material notch with the stress singularity exponent different from $\frac{1}{2}$. This paper deals with the experimental determination of the strength of adhesive connections and the selection of a proper surface treatment. A comparison of the experimentally determined strengths shows that the fracture mechanical approach constitutes a very useful tool for designers. Unstable fracture propagation can be determined even before time consuming and expensive prototyping, which reduces time and cost during the product development phase.

2. Experimental determination of strength of adhesive connection

As a part of the strength evaluation of aluminum bonding, surface pretreatment with different states of the substrates was investigated. The goal was to compare different ways of pretreatment of the commercial adhesive system Huntsman Araldite XD 4815 / XB 5323.

The mechanical properties of the adhesive as a function of temperature were measured by the dynamic mechanical analysis (DMA). This method allows to measure reversible (elastic) and irreversible (viscous) responses of polymers to deformation depending on the temperature and the deformation rate. The storage modulus (E') and the loss modulus (E'') were measured for desired range of temperature ($E'=3000$ MPa for ambient temperature). The evaluation of the glass transition temperature (T_g) is preferably above the maximum of E'' , which is in this

* Jakub Korbel: ABB Schweiz; Corporate Research; 5405 Baden-Daettwil, Switzerland; tel.: +41585868061; e-mail: jakub.korbel@ch.abb.com

** Prof. RNDr. Zdeněk Knésl, CSc, Jan Klusák Ph.D.; Ústav fyziky materiálů AV ČR; Žitkova 22, 616 62 Brno; tel: +420.532 290 358; e-mail: knesl@ipm.cz, klusak@ipm.cz

case 83°C. It is quite obvious that above the T_g , the adhesive reaches a rubbery state which is characterized by a viscoelastic behavior. Since the main focus of this work is prediction of brittle fracture, all residual stresses above the T_g were neglected for further numerical analysis. The starting temperature for thermal loading is then T_g and the residual stresses are then generated by different thermal expansions of the adhesive and adherent.

The investigation of the resistance of the aluminum-epoxy-bonding with various surface treatment conditions was conducted in accordance with DIN EN 1465. As an adhesive, the two-component commercial epoxy adhesive Huntsman Araldite XD 4815 / XB 5323 was used. The aluminum substrates were pretreated in various ways (anodizing process with or without sealing the oxide layer, sand blasted surfaces and bright rolled). The dimensions of the substrates were 25 mm × 100 mm × 3 mm. Two plates of the substrate were glued together (Figure 1). The overlap was 12 mm and the thickness of the adhesive was 0.15 mm.

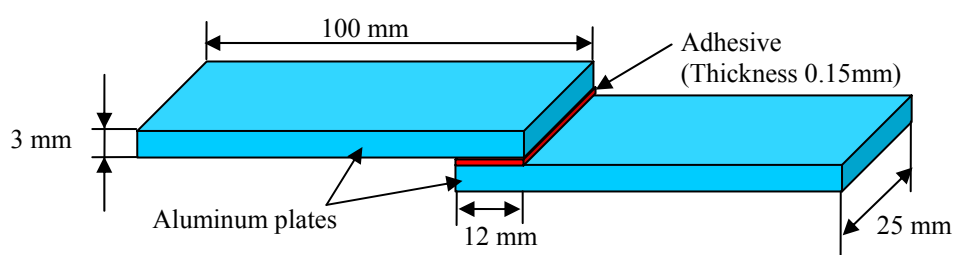


Figure 1 Dimensions of the test specimen for the determination of tensile lap shear strength according to DIN EN 1465

The determination of the maximum tension stress was made on a Zwick universal testing machine of type Z020 in accordance with DIN EN 1465. Five specimens of each surface treatment were tested. The test rate was 5mm/min. Standard wedge clamping was used.

Two different types of the failure were observed:

- Cohesive failure, where the fracture propagates on the interface between adhesive and adherent. This type of the failure is caused by poor adhesion and was characteristic by lower strength of the adhesive connection.
- Inter adhesive failure, where the fracture propagates through the adhesive. Higher strength (average critical stress 95 MPa) was in this case observed and this type of the failure will be analyzed in the following chapters of the paper.

3. Prediction of unstable crack propagation of the specimens

The step change of material parameters near the free edge of the adhesive joint induced singular stress distribution. The singular stress concentrator is modeled here using a bi-material notch with the stress singularity exponent different from 1/2. Generalized fracture mechanics approach provides reliable prediction of unstable crack propagation from the singular stress concentrator on the basis of the approaches originally developed for a crack in isotropic homogenous materials. Expressions for stress distribution in the vicinity of singular stress concentrators can be determined by the following equation:

$$\sigma_{ijm} = \sum_{k=1}^n \frac{H_k}{\sqrt{2\pi}} \cdot r^{-p_k} \cdot F_{ijkm}(\theta, \text{geom}, m, \dots) \quad (1)$$

where n is a number of corresponding singular terms, σ_{ijm} are the stress components respecting the polar coordinates $i, j = r, \theta$, the subscript m differentiates the materials 1 and 2 (adhesive and aluminum) where the stresses are determined, H_k are the generalized stress intensity factors (GSIFs), F_{ijkm} calibrating functions, r the distance from the notch tip and p_k are the exponents of the stress singularities.

The estimation of p for bi-material notches has been published in literature, e.g. Z.Q. Qian (2001) and will not be repeated here. For the example dealt with below (see

Figure 2) two singular terms occur, corresponding to the two exponents p_1 and p_2 , and the two GSIFs H_1, H_2 . The GSIFs are determined for concrete specimen geometry and material combination and for given boundary conditions on the basis of the results of numerical calculations by means of the finite element method (FEM). The calibrating functions F_{ijkm} for the studied case of the bi-material notch are as follows (Klusák et al., 2007):

$$F_{rrkm} = (2 - p_k)(-a_{mk} \sin((2 - p_k)\theta) - b_{mk} \cos((2 - p_k)\theta) + 3c_{mk} \sin(-p_k\theta) + 3d_{mk} \cos(-p_k\theta))$$

$$F_{\theta\theta km} = (p_k^2 - 3p_k + 2)(a_{mk} \sin((2 - p_k)\theta) + b_{mk} \cos((2 - p_k)\theta) + c_{mk} \sin(-p_k\theta) + d_{mk} \cos(-p_k\theta))$$

$$F_{r\theta km} = (2 - p_k)(-a_{mk} \cos((2 - p_k)\theta) + b_{mk} \sin((2 - p_k)\theta) + c_{mk} \cos(-p_k\theta) - d_{mk} \sin(-p_k\theta))$$

The coefficients $a_{mk}, b_{mk}, c_{mk}, d_{mk}$ for $k = 1, 2$ are known parameters depending on the material combination and notch geometry, and they are normalized in the way that for the case of a crack in a homogeneous material ($p_I = p_{II} = 0.5$) the GSIFs H_1 and H_2 pass to SIFs K_I and K_{II} .

3.1. Failure prediction

For the classical linear elastic fracture mechanics, the criterion for unstable crack propagation loaded by the normal mode is well known:

$$K_I < K_{IC} \quad (2)$$

where K_{IC} is fracture toughness, which is a material parameter and has to be measured. We can construct the failure criterion for a bi-material notch in a similar way (Knésl et al., 2007):

$$H_k < H_{IC}(K_{IC}) \quad (3)$$

The values of GSIF H_k are calculated by a numerical solution. The critical value of the GSIF H_{IC} depends on the critical material characteristic K_{IC} . The maximum values of tangential stress (see Figure 4) indicate that the fracture will propagate into the aluminum plates. In the reality a crack was propagating in the adhesive or at the interface in the case of poor adhesion between the adhesive and adherent (C1, B32 samples). This behavior is caused by the difference in fracture toughness of aluminum, the adhesive and the interface. Since the fracture of most of the samples occurred in the adhesive, this case will be further analyzed.

For estimation of the generalized fracture toughness (GFT) two methods were selected. The criterion based on the mean values of tangential stress (MTS) is defined by the following equation:

$$H_{1C} = \frac{2K_{IC}}{\frac{d^{0.5-p_1}}{1-p_1} F_{\theta\theta 1m}(\theta_0) + \Gamma_{21} \frac{d^{0.5-p_2}}{1-p_2} F_{\theta\theta 2m}(\theta_0)} \quad (4)$$

where $\Gamma_{21} = H_2/H_1$, and d is a micromechanical parameter which has to be chosen in dependence on the mechanism of rupture, see Klusák et al. (2007). The second method for

estimation of GFT is based on the strain energy density factor (SEDF), which was proposed by Sih (1977). GFT is then defined by the following relation; see Klusák et al. (2007):

$$H_{1C} = 2K_{IC,m} \sqrt{\frac{k_m}{\frac{d^{1-2p_1}}{2-2p_1} U_{1m} + \frac{d^{1-2p_2}}{2-2p_2} \Gamma_{21}^2 U_{2m} + \frac{d^{1-p_1-p_2}}{2-p_1-p_2} 2\Gamma_{21} U_{12m}}} \quad (5)$$

where $k_m = (1-\nu_m)/(1+\nu_m)$ for plane stress or $k_m = (1-2\nu_m)$ for plain strain, ν_m is Poisson's ratio of material $m = 1, 2$ and U_{1m}, U_{2m}, U_{12m} are known functions.

For the sake of simplification and better interpretation of the results of the stress concentrator assessment the critical applied load can be expressed as:

$$\sigma_{crit} = \sigma_{appl} \frac{H_{1C}}{H_1(\sigma_{appl})} \quad (6)$$

where σ_{appl} is the applied stress used in numerical calculations of H_1 and H_2 . Unstable crack propagation will not occur if the applied stress is lower than the critical value.

$$\sigma_{appl} < \sigma_{crit} \quad (7)$$

3.2. Numerical model

The stress field computation was carried out by the commercial FEM code Abaqus. The attention was initially focused on residual stresses caused by curing conditions at high temperatures. Since the solidification occurs at a higher temperature, the consequent temperature drop to the ambient temperature leads to a generation of the residual stresses caused by different thermal expansions of a polymeric adhesive and aluminum. As mentioned before, above the glass transition temperature T_g , the adhesive reaches a rubbery state which is characterized by a viscoelastic behavior and the stress relaxation is significant in time. For an estimation of the residual stresses it was assumed that all stresses generated above T_g were negligible. This significantly simplifies the analysis as the viscoelastic behavior is not then considered. Coupled temperature-displacement analysis was performed as a first step of the analysis. The temperature dropped from T_g (83°C) to ambient temperature (23°C). Since the geometry is simple, only 2D simulation was performed under plain strain conditions, considering ideal adhesion between the adhesive and adherent. The second step of the analysis reflects the condition of the tensile test. The boundary conditions are shown in Figure 2. On one side all degrees of freedom (DOF) were limited (fixed clamp) and on the other side only degrees of freedom perpendicular to load were limited (movable clamp).

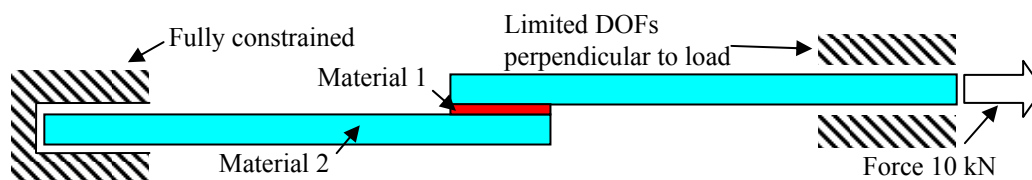


Figure 2 Boundary conditions for structural analysis

The material characteristics were taken as follows: Material 1 – the adhesive – Young's modulus $E_1 = 3000$ MPa, Poisson's ratio $\nu_1 = 0.34$, fracture toughness $K_{IC} = 2$ MPa.m^{1/2}. Material 2 – aluminum – Young's modulus $E_2 = 70000$ MPa, Poisson's ratio $\nu_2 = 0.33$, fracture toughness $K_{IC} = 24$ MPa.m^{1/2}. The FEM mesh density is visible in Figure 3. In order

to compute the stress field with a minimal numerical error, refinement of the mesh was applied in the vicinity of the notch tip (element size 1e-6 m).

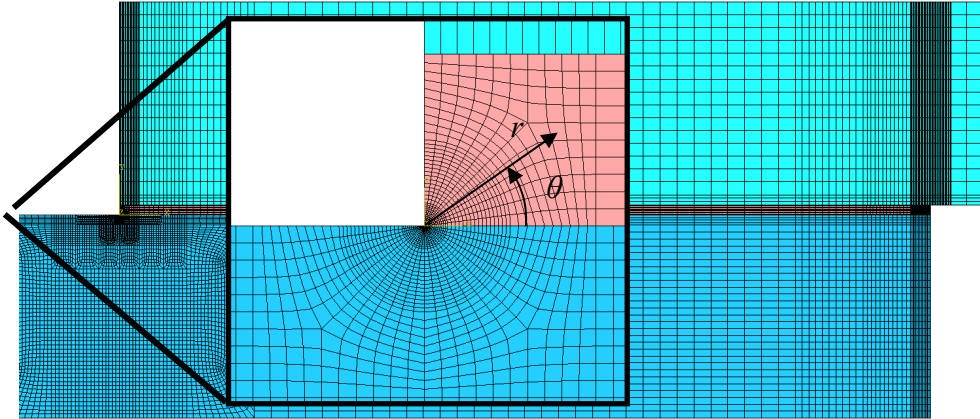


Figure 3 Mesh density

The first results (tangential stresses around the notch tip at a distance of 1e-5 m) of the coupled temperature-displacement and the structural analysis were compared with the results of purely structural analysis without considering residual stresses (see Figure 4). The influence of residual stresses in the specific case is negligible. Considering the residual stresses, the maximum tangential stress in the aluminum is approximately 1% higher. Moreover, the tangential stress in the adhesive is about 5% lower if the residual stresses are considered. Due to these findings, the residual stresses for this specific example can be neglected.

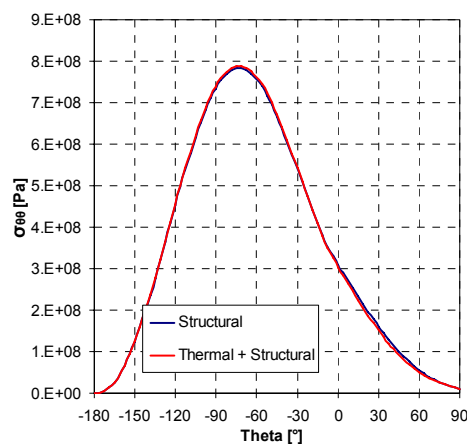


Figure 4 Comparison of tangential stresses

3.3. Estimation of the fracture parameters

To calculate the GSIFs H_1 and H_2 , the direct method was applied. The method is based on the extraction of tangential stresses from two separate paths leading from the notch tip into a material. The first path was selected in the direction $\theta_1 = -75^\circ$ where the tangential stress has its maximum. The angle of the second was chosen $\theta_2 = -37.5^\circ$. By using the equation (1) the GSIFs can then easily be calculated on the paths. Extrapolation of the linear regions of the GSIF values into the notch tip ($r = 0$) provides the desired values of H_1 and H_2 (Figure 5).

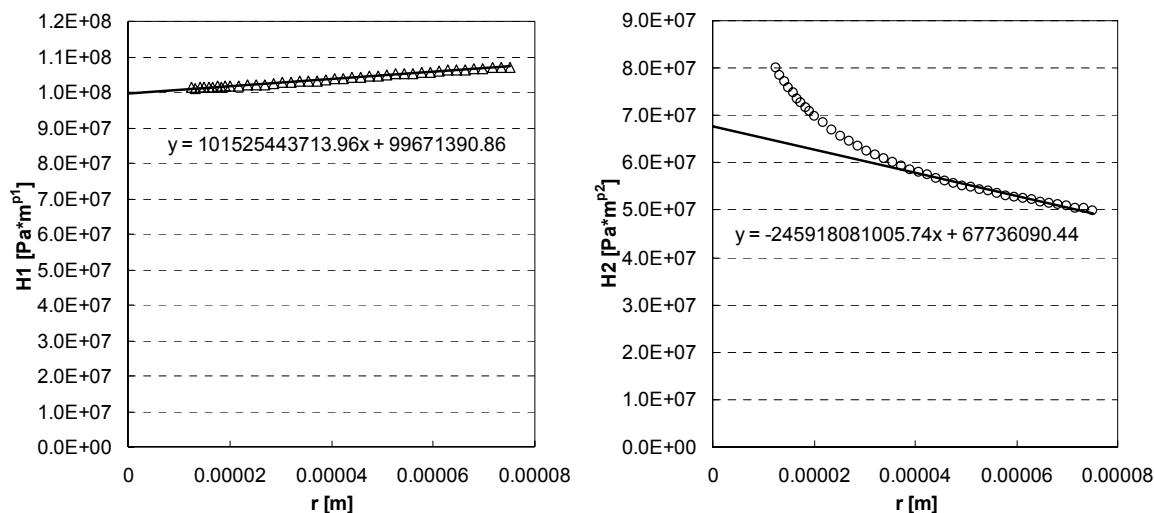


Figure 5 Extrapolation of the GSIF values

Knowing the GSIFs H1 and H2 and their critical values, see the paragraph 3.1, the critical applied loads can be ascertained. The results of the calculated critical stress of the specimen as a function of the parameter d are shown in Figure 6. Both methods (MTS and SEDF) are directly compared. The SEDF method provides slightly lower values of the critical stress. The parameter d reflects the mechanism of the rupture and for polycrystal materials like steel should be chosen in a range of 2 – 5 times the size of grains. For polymeric thermosetting materials the magnitude of the parameter d has not been determined yet, therefore critical stress is provided in a reasonable range of the magnitude of the parameter d .

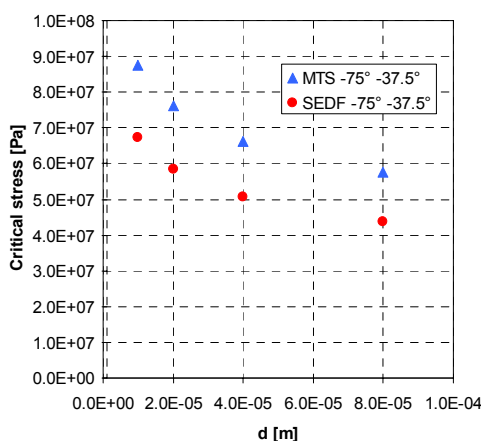


Figure 6 Critical stress as a function of parameter d

4. Conclusions

Measurements of the failure of adhesive joint specimens loaded by tensional stress were performed. The experimental results were compared with numerically estimated values of the failure stress computed based on the estimation of the generalized stress intensity factor and application of two failure criterions (MTS and SEDF). Maximal critical stress for each criterion varies and for both cases is lower than real measured critical stress of not aged samples (average 95 MPa). This is mainly due to the fact that the numerical simulation assumes the worst case scenario of an utterly sharp edge of the notch. Despite the fact that the

free edge of the samples was cleaned and excessive adhesive was removed from the tip before testing, certain finite radius remained in the notch tip. However numerically calculated values of the critical stress provide a conservative evaluation of the allowed loading of adhesive joints and the same approach can be used for more complex geometries.

5. Acknowledgements

The authors are grateful for financial support through the Research projects of the Academy of Sciences of the Czech Republic (1QS200410502 and AVOZ20410507) and the project of the Czech Science Foundation (101/08/0994).

6. References

- Sih, G.C., (1977) A special theory of crack propagation, *Mechanics of Fracture – Methods of Analysis and Solutions of Crack Problems*, Noordhoff International Publishing, Leyden, The Netherlands.
- Qian, Z.Q., (2001) On the evaluation of wedge corner stress intensity factors of bi-material joints with surface tractions. *Computers and Structures*, 79 53-64.
- Knésl, Z., Klusák, J., Náhlík, L., (2007) Crack initiation criteria for singular stress concentrations. Part I: A universal assessment of singular stress concentrations. *Engineering MECHANICS*, vol. 14, No. 6, p. 399-408.
- Klusák, J., Knésl, Z., Náhlík, L., (2007) Crack initiation criteria for singular stress concentrations. Part II: Stability of sharp and bi-material notches. *Engineering MECHANICS*, vol. 14, No. 6, p. 409-422.